



Aalborg Universitet

AALBORG UNIVERSITY
DENMARK

On the fitness landscapes of interdependency models in the travelling thief problem

El Yafrani, Mohamed; Martins, Marcella; Delgado, Myriam; Luders, Ricardo; Nielsen, Peter; Wagner, Markus

Published in:

GECCO 2022 Companion - Proceedings of the 2022 Genetic and Evolutionary Computation Conference

DOI (link to publication from Publisher):

[10.1145/3520304.3528798](https://doi.org/10.1145/3520304.3528798)

Creative Commons License
CC BY 4.0

Publication date:
2022

Document Version
Early version, also known as pre-print

[Link to publication from Aalborg University](#)

Citation for published version (APA):

El Yafrani, M., Martins, M., Delgado, M., Luders, R., Nielsen, P., & Wagner, M. (2022). On the fitness landscapes of interdependency models in the travelling thief problem. In *GECCO 2022 Companion - Proceedings of the 2022 Genetic and Evolutionary Computation Conference* (pp. 188-191). Association for Computing Machinery. <https://doi.org/10.1145/3520304.3528798>

General rights

Copyright and moral rights for the publications made accessible in the public portal are retained by the authors and/or other copyright owners and it is a condition of accessing publications that users recognise and abide by the legal requirements associated with these rights.

- Users may download and print one copy of any publication from the public portal for the purpose of private study or research.
- You may not further distribute the material or use it for any profit-making activity or commercial gain
- You may freely distribute the URL identifying the publication in the public portal -

Take down policy

If you believe that this document breaches copyright please contact us at vbn@aub.aau.dk providing details, and we will remove access to the work immediately and investigate your claim.

On the Fitness Landscapes of Interdependency Models in the Travelling Thief Problem

Mohamed El Yafrani
Aalborg University
Denmark
mey@mp.aau.dk

Marcella Scoczynski
Federal University of Technology
Paraná (UTFPR)
Brazil
marcella@utfpr.edu.br

Myriam R. B. S. Delgado
Federal University of Technology -
Paraná (UTFPR)
Brazil
myriamdelg@utfpr.edu.br

Ricardo Lüders
Federal University of Technology -
Paraná (UTFPR)
Brazil
luders@utfpr.edu.br

Peter Nielsen
Aalborg University
Denmark
peter@mp.aau.dk

Markus Wagner
The University of Adelaide
Australia
markus.wagner@adelaide.edu.au

ABSTRACT

Since its inception in 2013, the Travelling Thief Problem (TTP) has been widely studied as an example of problems with multiple interconnected sub-problems. The dependency in this model arises when tying the travelling time of the “thief” to the weight of the knapsack. However, other forms of dependency as well as combinations of dependencies should be considered for investigation, as they are often found in complex real-world problems. Our goal is to study the impact of different forms of dependency in the TTP using a simple local search algorithm. To achieve this, we use Local Optima Networks, a technique for analysing the fitness landscape.

KEYWORDS

Local Optima Networks, Basins of attraction, Travelling Thief Problem, Interdependency models

1 MOTIVATION

Many real-world optimisation problems can be modelled as a combination of multiple sub-problems with internal dependencies [2]. These dependencies can be formulated as equations or inequalities to connect the sub-problems. This class of problems are referred to as problems with multiple interdependent components [1] or multi-hard problems [13].

Due to the lack of a good benchmarking model to study multi-hard problems, the travelling thief problem was introduced by Bonyadi et al. [1] as a combination of the Travelling Salesman Problem and the Knapsack Problem. A simplified formulation was then introduced by Polyakovskiy et al. [12] in order to have a version that is more focused on the interdependency aspect. Since then, several papers introduced solution methods (e.g., [3, 5, 10, 14]), while only few researchers tried to analyse the problem itself empirically and theoretically (e.g., [6, 15, 16]). Therefore, the goal of this study is to reduce the gap in the problem analysis and provide insights into the problem search landscape.

The standard TTP formulation in [12] considers a combination of the Travelling Salesman Problem (TSP) and the Knapsack Problem (KP). The problem considers a set of items

scattered in different cities, and a thief that should visit each city exactly once, stealing items on the way and returning to the starting city, while trying to maximise his gain. The dependency in this formulation is modelled by penalising the travel velocity with the knapsack load. While this is a useful model to reflect the dependencies faced in some realistic problems, other problems can embed other – potentially more complex – forms of interdependency, where multiple dependency equations or inequalities can be combined [2].

Herein, we present preliminary results on 4 dependency models of the TTP. Specifically, we use Local Optima Networks (LONs) [11] – a method for fitness landscape analysis – to assess the difficulty of the standard TTP model and other three proposed models of dependency, including a dependency-free model. The reported results show initial insights into the impact of adding more interdependency equations and the influence of instance features on the difficulty of solving multi-hard problems with local search heuristics.

2 PROPOSED APPROACH

2.1 Background on Local Optimal Networks

In the following, we analyse TTP dependency models based on Local Optima Networks (LONs), which is a fitness landscape technique. LONs provide a compressed and simplified version of the search space, represented as a graph where nodes are the local optima and edges are the possible search transitions among optima depending on a given local search operator [11]. Each local optimum has an associated basin of attraction composed of all solutions that converge to it when applying a local search heuristic.

As shown in Figure 1, the basin of attraction associated with a local optima i (red dot) is the set $B_i = \{s \in S, \mathcal{A}(s) = i\}$ with cardinality $|B_i|$, where s is a solution (black dot) from the solution space S , and \mathcal{A} is the local search procedure. A connection exists (blue dashed lines) between two local optima nodes if at least one solution in one basin has a neighbour solution in the other basin using the local search (neighbourhood) operator.

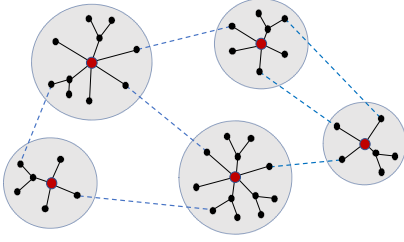


Figure 1: An example of a LON with basins of attraction.

While many approaches to solving the TTP exist, only few rigorously analyse the difficulty of the problem based on the problem features. Wu et al. [15] varied the renting rate parameter in an attempt to create hard-to-solve instances. El Yafrani et al. [6] used the local optima network representation to better understand the TTP’s search space structure when using a local search heuristic joining the TSP and KP neighbourhoods [4]. The same representation is adopted by [16], who analysed fitness landscape characteristics from smaller instances of the problem, investigating the effectiveness of operators and metaheuristics that use local search.

In this paper, we extract LONs from multiple enumerable TTP instances using a neighbourhood search algorithm. This is done to investigate the impact of the problem features on the performance of local search by studying the topological structure of the problem search space. The pseudocode of the local search is listed in Algorithm 1 where $F(\cdot)$ is the TTP objective function, $\mathcal{N}_{TSP}(\cdot)$ and $\mathcal{N}_{KP}(\cdot)$ represent the neighbourhood functions for the TSP and KP components respectively. In the context of this study, we consider the local search named J2B [4] which uses the 2-OPT neighbourhood operator to generate $\mathcal{N}_{TSP}(\cdot)$ and the one-bit-flip operator for the $\mathcal{N}_{KP}(\cdot)$ neighbourhood.

Algorithm 1 Joint neighbourhood search algorithm

```

1:  $s \leftarrow$  initial solution
2: while there is an improvement do
3:   for each  $s^* \in \mathcal{N}_{TSP}(s)$  do
4:     for each  $s^{**} \in \mathcal{N}_{KP}(s^*)$  do
5:       if  $F(s^{**}) > F(s)$  then
6:          $s \leftarrow s^{**}$ 

```

While approaches with a sequential neighbourhood structure (iterating between the sub-problem neighbourhoods instead of combining them as in Algorithm 1) report better results [3, 10], they would result in a new LON for each sub-problem whenever the solution changes for the other sub-problem. Thus, the joint structure in Algorithm 1 was chosen due to this limitation.

2.2 Interdependency models

2.2.1 Standard model of interdependency. The standard TTP model, TTP_A (as per [12]) is formulated as follows: given a set of n cities, the associated matrix of distances d_{ij} , and a set of

m items distributed among these cities; each item k is related with a profit p_k and a weight w_k . The problem states that a thief should visit all the cities exactly once, stealing items on the road, returning to the starting city. The knapsack capacity is denoted W , the renting ratio, denoted R , dictates how much the thief should pay at the end of the travel with respect to the travel time, and v_{max} and v_{min} represent the maximum and minimum velocities respectively. Furthermore, each item is available in only one city, and $a_k \in \{1, \dots, n\}$ contains the reference of item k to the corresponding city.

A TTP solution is represented by the tour $x = (x_1, \dots, x_n)$, a vector which contains the ordered list of cities; and the picking plan $z = (z_1, \dots, z_m)$, a binary vector coding the status of items (1 for "packed", and 0 for "not packed").

The TTP was designed considering that the speed of the thief changes according to the knapsack weight, which makes the sub-problems mutually dependent. Therefore, the thief’s velocity at city x is defined in Equation 1.

$$v_x = v_{max} - K \cdot w_x^* \quad (1)$$

where $K = (v_{max} - v_{min})/(W)$ is a constant value and w_x^* is the weight of the knapsack at city x .

We note $g(z) = \sum_k p_k z_k$, s.t. $\sum_k w_k z_k \leq W$ as the total items value and $f(x, z) = \sum_{i=1}^{n-1} t_{x_i, x_{i+1}} + t_{x_n, x_1}$ as the total travel time, where $t_{x_i, x_{i+1}} = d_{x_i, x_{i+1}}/v_{x_i}$ is the travel time from x_i to x_{i+1} .

The objective is to maximise the total gain, $F_A(x, z) = g(z) - R \cdot f(x, z)$, by finding the best tour x and picking plan z .

2.2.2 Extended models of interdependency. Here, we propose three additional models with different types of interdependencies.

The first model, TTP_0 , does not include any dependency, and it will serve for comparison with the other models. The objective function for TTP_0 is $F_0(x, z) = g(z) - R \cdot f(x)$.

The second TTP model, TTP_B , considers that the value of the items drops by time, and it does not consider the velocity-load dependency in Equation 1. Therefore the total value $g(x, z)$ depends on the tour too. The value of an item k drops from p_k to $p_k^{final} = p_k \cdot \mathcal{D}^{\lceil \frac{T_k}{T_0} \rceil}$, where $\mathcal{D} \in [0.1, 0.99]$ is the dropping rate, and T_k is the carrying time. To focus on the dependency analysis, we consider a linear combination of both objectives as $F_B(x, z) = g(x, z) - R \cdot f(x)$.

The last model, TTP_C , considers both types of dependency and its objective function is $F_C(x, z) = g(x, z) - R \cdot f(x, z)$.

The item value drop idea was introduced in [1] to create a bi-objective version of the TTP (TTP_2). Here, we also use this idea in TTP_B and TTP_C , however both are single-objective.

For the purpose of efficient implementations of neighbourhood-searching algorithms, the solution evaluation algorithms for TTP_A , TTP_B and TTP_C have the same worst-case complexity. However, the actual computation time for TTP_A and TTP_B can be significantly improved through caching when generating neighbouring solutions [5, 10]. Such an approach is more difficult to achieve under the added item drop equation in TTP_C .

3 EXPERIMENTAL RESULTS AND DISCUSSION

Herein, we present the results of the empirical study of the the four models of interdependency. The instance are generated based on [1, 12] and categorised based on the following features:

- **Profit-value correlation (\mathcal{T}):** This describes the correlation of the weight (w_k) and profit (p_k) of each item k . The TTP library addressed here considers three correlations, namely, *uncorrelated* (u), *uncorrelated with similar weight* (usw), and *bounded strongly correlated* (bsc).
- **Knapsack capacity class (\mathcal{C}):** This feature is a factor occurring in the maximum weight of the knapsack which is given by $W = \frac{C}{11} \sum_{j=1}^m w_j$, where $C \in \{2, 5, 10\}$ and $\frac{C}{11}$ is applied as a limit for W , i.e., class $C = 10$ enlarges W around to 90%, and more objects can be added in the knapsack [12].
- **Item value dropping rate (\mathcal{D}):** This feature determines the rate at which the items lose value through time, and ranges between 0 and 1. This feature is used to determine the value of an item k at the end of the travel as follows $p_i = D^{\lfloor \frac{T_k}{T_0} \rfloor}$, where T_k is the total time that the item k has been carried.

We consider small instances to generate the local optima networks and identify the basins of attractions. Small instances have been chosen because the enumeration and study of the standard ones are impractical. The addressed instances contain 7 cities and 6 items (one per city, except for the starting one) and are generated following the guidelines by Polyakovskiy et al. [12]. The renting rate is given by $R = (g(Z_{opt}))/f(X_{opt}, Z_{opt})$, where Z_{opt} and X_{opt} represent the optimal picking plan and the optimal tour respectively for the instances considered here.

Table 1: LON metrics for TTP_0

\mathcal{T}	\mathcal{C}	\bar{n}_v	\bar{n}_e	\bar{C}	\bar{C}_r	\bar{l}	$ \mathcal{B} $
u	2	1356875	1996510676	0.44 _{0.17}	0.05 _{0.05}	2.22 _{0.24}	6 ₅
	5	26781752	7224042094	0.59 _{0.13}	0.04 _{0.05}	2.17 _{0.19}	12 ₁₀
	10	413379	1632918362	0.68 _{0.11}	0.34 _{0.26}	1.68 _{0.27}	274 ₂₇₃
usw	2	4320 ₀	52050 ₀	0.31 ₀	0.01 ₀	2.4 ₀	1 ₀
	5	10800 ₀	260482 ₀	0.26 ₀	0 ₀	2.58 ₀	1 ₀
	10	3374 ₂₅₅	157378 ₁₁₀₂₆	0.36 _{0.01}	0.03 ₀	2.21 _{0.03}	14 ₁
bsc	2	2040826	2853911355	0.32 _{0.09}	0.03 _{0.04}	2.32 _{0.17}	3 ₃
	5	33993204	11692979643	0.40 _{0.11}	0.08 _{0.09}	2.19 _{0.28}	16 ₁₈
	10	781517	5283932613	0.65 _{0.11}	0.30 _{0.23}	1.72 _{0.25}	112 ₁₁₀

Table 2: LON metrics for TTP_A

\mathcal{T}	\mathcal{C}	\bar{n}_v	\bar{n}_e	\bar{C}	\bar{C}_r	\bar{l}	$ \mathcal{B} $
u	2	483410	83246074	0.60 _{0.16}	0.25 _{0.3}	1.89 _{0.4}	64147
	5	10574	30132496	0.85 _{0.09}	0.58 _{0.25}	1.42 _{0.24}	495635
	10	2519	398530	0.97 _{0.05}	0.95 _{0.09}	1.05 _{0.09}	27771950
usw	2	1643770	214539261	0.50 _{0.04}	0.02 _{0.01}	2.31 _{0.06}	4 ₂
	5	30541421	9740432996	0.57 _{0.05}	0.03 _{0.03}	2.15 _{0.12}	7 ₄
	10	12517	55591379	0.84 _{0.01}	0.70 _{0.01}	1.30 _{0.01}	37062
bsc	2	1183814	1743910774	0.51 _{0.14}	0.12 _{0.21}	2.11 _{0.34}	1324
	5	7761718	2705748137	0.76 _{0.12}	0.49 _{0.28}	1.55 _{0.35}	134119
	10	5821	15371027	0.92 _{0.04}	0.87 _{0.07}	1.13 _{0.07}	836276

Table 3: LON metrics for TTP_B

\mathcal{T}	\mathcal{C}	\mathcal{D}	\bar{n}_v	\bar{n}_e	\bar{C}	\bar{C}_r	\bar{l}	$ \mathcal{B} $
u	2	0.9	741634	104328838	0.57 _{0.21}	0.17 _{0.25}	2.02 _{0.39}	33 ₄₄
		0.95	1263823	187329734	0.50 _{0.18}	0.05 _{0.05}	2.16 _{0.18}	7 ₁₀
		0.98	626513	97886313	0.53 _{0.18}	0.17 _{0.24}	1.99 _{0.35}	24 ₄₀
usw	5	0.9	303192	120879042	0.76 _{0.06}	0.34 _{0.2}	1.66 _{0.21}	104 ₈₀
		0.95	944773	3408329961	0.64 _{0.12}	0.21 _{0.25}	1.85 _{0.29}	67 ₈₀
		0.98	1247813	4180226987	0.61 _{0.07}	0.08 _{0.06}	1.99 _{0.11}	27 ₂₁
bsc	10	0.9	6728	19551387	0.90 _{0.05}	0.82 _{0.1}	1.18 _{0.1}	777 ₃₃₇
		0.95	10557	40723690	0.83 _{0.05}	0.69 _{0.13}	1.31 _{0.13}	517 ₂₀₃
		0.98	380412	1965924222	0.75 _{0.16}	0.46 _{0.33}	1.54 _{0.33}	419 ₄₁₉
u	2	0.9	3761443	460095229	0.45 _{0.06}	0.01 ₀	2.36 _{0.02}	1 ₀
		0.95	428355	51701537	0.33 _{0.02}	0.01 ₀	2.39 _{0.01}	1 ₀
		0.98	43200	5204969	0.31 ₀	0.01 ₀	2.4 ₀	1 ₀
usw	5	0.9	2789391	915428516	0.60 _{0.01}	0.02 ₀	2.16 _{0.04}	6 ₁
		0.95	6470467	17235210217	0.47 _{0.01}	0.01 ₀	2.30 _{0.01}	2 ₀
		0.98	9947708	24519314408	0.33 _{0.03}	0 ₀	2.43 _{0.02}	2 ₀
bsc	10	0.9	1675	8527300	0.81 ₀	0.62 _{0.01}	1.38 _{0.01}	27 ₂₈
		0.95	51475	342475195	0.69 _{0.01}	0.26 _{0.04}	1.74 _{0.04}	90 ₁₃
		0.98	1473157	849407299	0.58 _{0.01}	0.08 _{0.01}	1.95 _{0.02}	3 ₃
u	2	0.9	1367985	1858010718	0.53 _{0.14}	0.15 _{0.25}	2.09 _{0.4}	15 ₂₈
		0.95	1003846	1963712444	0.49 _{0.14}	0.10 _{0.09}	2.05 _{0.25}	12 ₁₁
		0.98	1978932	2996313027	0.33 _{0.14}	0.05 _{0.1}	2.34 _{0.26}	8 ₁₇
bsc	5	0.9	560973	2076631803	0.77 _{0.13}	0.45 _{0.34}	1.57 _{0.38}	175 ₁₈₅
		0.95	1262597	6410030502	0.56 _{0.09}	0.13 _{0.13}	1.96 _{0.2}	24 ₂₅
		0.98	33512567	12401489315	0.46 _{0.13}	0.08 _{0.14}	2.17 _{0.29}	18 ₂₈
u	10	0.9	8537	33511979	0.91 _{0.05}	0.85 _{0.09}	1.15 _{0.09}	725 ₆₄₄
		0.95	212109	138498907	0.82 _{0.07}	0.65 _{0.19}	1.35 _{0.19}	283 ₁₈₅
		0.98	462444	2889325806	0.75 _{0.14}	0.52 _{0.31}	1.49 _{0.32}	194 ₁₃₆

Table 4: LON metrics for TTP_C

\mathcal{T}	\mathcal{C}	\mathcal{D}	\bar{n}_v	\bar{n}_e	\bar{C}	\bar{C}_r	\bar{l}	$ \mathcal{B} $
u	2	0.9	276215	57284859	0.58 _{0.12}	0.25 _{0.17}	1.82 _{0.24}	28 ₂₉
		0.95	351234	58264307	0.65 _{0.17}	0.19 _{0.19}	1.90 _{0.27}	24 ₂₃
		0.98	191300	39527226	0.76 _{0.18}	0.54 _{0.3}	1.50 _{0.38}	105 ₁₀₃
usw	5	0.9	4018	777582	0.93 _{0.04}	0.88 _{0.09}	1.12 _{0.09}	658 ₃₉₀
		0.95	6373	20173582	0.91 _{0.08}	0.82 _{0.19}	1.17 _{0.19}	681 ₅₅₂
		0.98	7149	20721875	0.86 _{0.07}	0.69 _{0.17}	1.31 _{0.17}	632 ₆₃₆
bsc	10	0.9	208	216166	0.99 _{0.01}	0.99 _{0.02}	1.01 _{0.02}	2538 ₁₁₅₀
		0.95	198	200157	0.99 _{0.02}	0.98 _{0.02}	1.02 _{0.02}	2849 ₁₄₁₃
		0.98	2713	393350	0.97 _{0.03}	0.96 _{0.04}	1.04 _{0.04}	203 ₂₉₄₉
u	2	0.9	73093	106461026	0.41 _{0.03}	0.04 _{0.01}	2.25 _{0.03}	7 ₁
		0.95	816166	116191909	0.44 _{0.04}	0.04 _{0.01}	2.26 _{0.03}	6 ₁
		0.98	1060291	145043482	0.47 _{0.03}	0.03 _{0.01}	2.29 _{0.04}	5 ₂
usw	5	0.9	18077	97305706	0.79 _{0.06}	0.62 _{0.15}	1.38 _{0.15}	107 ₄₉
		0.95	408102	263837503	0.71 _{0.03}	0.33 _{0.07}	1.67 _{0.07}	41 ₁₁
		0.98	739319	3896713790	0.67 _{0.04}	0.18 _{0.1}	1.84 _{0.12}	26 ₁₃
bsc	10	0.9	257	305190	0.99 _{0.01}	0.99 _{0.02}	1.01 _{0.02}	1960 ₄₂₄
		0.95	523	1255165	0.95 _{0.01}	0.94 _{0.02}	1.06 _{0.02}	872 ₅₈
		0.98	4211	886499	0.97 _{0.01}	0.96 _{0.01}	1.04 _{0.01}	1137 ₂₅₆
u	2	0.9	426286	68193726	0.59 _{0.19}	0.24 _{0.34}	1.89 _{0.43}	36 ₆₅
		0.95	232219	49275598	0.69 _{0.14}	0.36 _{0.27}	1.69 _{0.33}	51 ₄₄
		0.98	505384	91197403	0.59 _{0.15}	0.22 _{0.25}	1.90 _{0.36}	31 ₄₀
bsc	5	0.9	6187	25396173	0.93 _{0.1}	0.88 _{0.19}	1.12 _{0.19}	697 ₄₀₈
		0.95	7934	21211170	0.87 _{0.08}	0.75 _{0.22}	1.25 _{0.22}	298 ₁₄₂
		0.98	21187	974910470	0.81 _{0.11}	0.56 _{0.31}	1.44 _{0.31}	252 ₂₃₀
u	10	0.9	268	338214	0.98 _{0.02}	0.98 _{0.02}	1.02 _{0.02}	1834 ₅₂₂
		0.95	4112	803418	0.96 _{0.03}	0.94 _{0.05}	1.06 _{0.05}	1197 ₄₃₁
		0.98	4821	1205929	0.95 _{0.03}	0.93 _{0.05}	1.07 _{0.05}	1105 ₅₃₅

During the instance generation process, the TSP component is fixed, i.e., the set of coordinates is the same for all the instances. We use three capacity classes $C \in \{2, 5, 10\}$, three dropping rates $\mathcal{D} \in \{0.9, 0.95, 0.98\}$ (for TTP_B and TTP_C), and all three correlation variants (u , usw , and bsc). This results in 9 classes for TTP_0 and TTP_A , and in 27 classes for TTP_B and TTP_C . For each class, 100 instances are generated, and the corresponding LONs are extracted to analyse their fitness landscapes.

Tables 1, 2, 3 and 4 show the graph metrics for the standard and extended models, with the subscript numbers representing standard deviations. The results in Tables 2 and 4 are aligned with the findings in [6] and can be summarised as follows. When the knapsack capacity is increased (higher C),

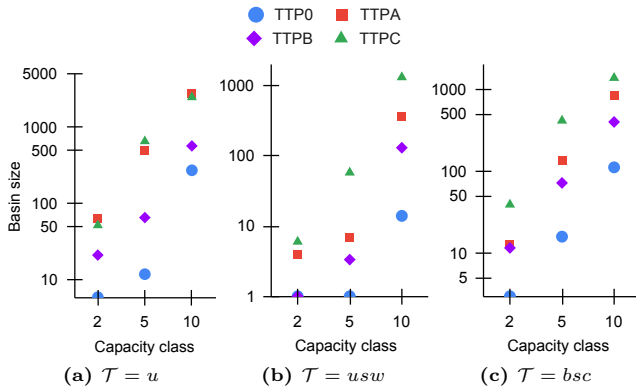


Figure 2: Comparison of the average basin sizes. For TTP_B and TTP_C the averages across the three D values is used

the number of nodes (\bar{n}_v) and edges (\bar{n}_e) decreases, while the basin size ($|\bar{B}|$) increases. This means that the landscape is easy to navigate when the knapsack capacity is large. This trend is sometimes broken when the values of items are uncorrelated with the weights, and the weights are similar ($\mathcal{T} = usw$).

The average path lengths (\bar{l}) are always small, which shows that the transition from a random local optimum to another is done through very few intermediate local optima. This fact, combined with the observation that the clustering coefficient (\bar{C}) is always higher than the clustering coefficient of the equivalent Erdős-Rényi random graph (\bar{C}_r), indicates that the LONs have small-world properties [8]. It is worth mentioning that when the LON has a small number of nodes, the corresponding random graph naturally has a high clustering coefficient (\bar{C}_r), which can be explained by the small number of combinations to connect the nodes.

In Tables 3 and 4, it is difficult to isolate the impact of changing the dropping rate (D). In Table 4, the most prominent trend is a positive correlation between D and the basin size $|\bar{B}|$. However, more samples over D are required to isolate the outliers if any and understand its impact.

Interestingly, in Figure 2, when comparing the basin sizes of all models, we observe that the basin sizes of TTP_0 are mostly smaller than the remaining models. This is suggesting that the models with dependencies result in landscapes that are easier to navigate compared to the dependency-free model TTP_0 .

To further investigate the difficulty of the different models, we consider Spearman’s correlation coefficients between the fitness and basin size for all models, where the average is calculated using Fisher z-transformation [7]. The correlations are as follows: $\rho(TTP_0) = 0.61$, $\rho(TTP_A) = 0.79$, $\rho(TTP_B) = 0.74$, $\rho(TTP_C) = 0.80$, and the associated scatter plots are shown in Figure 3. There is a positive correlation between the fitnesses and basin sizes for all 4 models, showing that larger basins tend to have a higher fitness. The correlation is

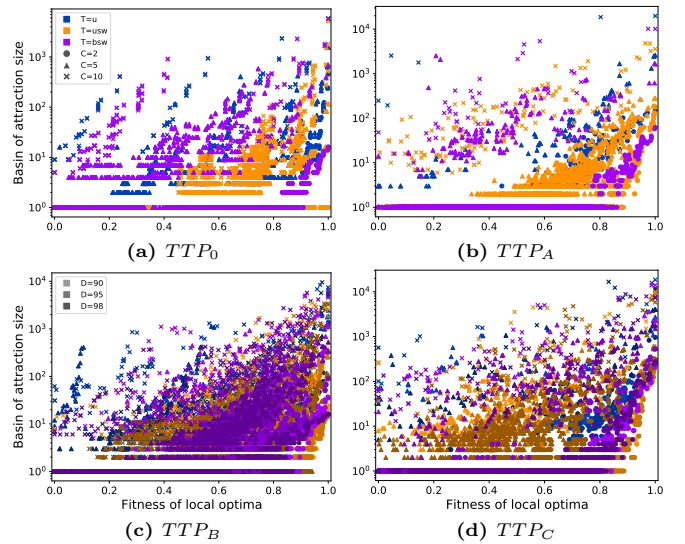


Figure 3: Fitness-basin size correlations. Shown for one random instance per category.

clearly the weakest for TTP_0 , i.e., it appears to be the most difficult there to find an optimal solution. This correlation can be seen for individual categories in Figure 3.

In summary, it is surprising that the introduction of interdependencies appears to make the problem easier for the given algorithm. We can only speculate about the reasons. Firstly, it might be that the joint neighbourhood search induces unnecessary complexity to the TTP_0 landscapes. Indeed, there is no interdependency in TTP_0 , i.e., the instances can simply be solved by solving the sub-problems separately. Secondly, maybe our analyses are inadequate, and new powerful tools are needed for characterising landscapes.

4 CONCLUSION

In this paper we have investigated the impact of different forms of dependency on the difficulty of solving problems with multiple interconnected sub-problems using local search. We considered the Travelling Thief Problem (TTP) as our study case and investigated three extended models embedding other forms of dependency, and compared it to the standard TTP model by analysing how dependency impacts the solution landscape of the problem.

The analysis was conducted on enumerable instances using Local Optima Networks (LONs) and topology metrics for a local search algorithm which combines the TSP and KP neighbourhoods. The preliminary results gave us some insights on the impact of the dependency equations to the standard TTP. Specifically, the addition does not appear to result in more difficult search landscapes for the considered algorithm.

Nevertheless, this study has some limitations and aspects that should be further investigated. Firstly, joint neighbourhood search algorithms are not the most efficient in practice

due to their high computational complexity. Thus, the analysis does not necessarily generalise to other types of local search with a sequential neighbourhood structure. Along similar lines, our results might not carry over to non-enumerable instances; however, if we investigate larger instances, the characteristics of the sampled LONs can be highly susceptible to the sampling approach [9]. Secondly, the item drop feature (\mathcal{D}) should be further investigated to better isolate its impact. Lastly, to overcome the limitations induced by LONs and composite structure of the TTP, regression (cost) models may be able provide additional insights on the behaviour of (meta-)heuristics on the TTP models.

REFERENCES

- [1] Mohammad Reza Bonyadi, Zbigniew Michalewicz, and Luigi Barone. 2013. The travelling thief problem: The first step in the transition from theoretical problems to realistic problems. In *2013 IEEE Congress on Evolutionary Computation*. IEEE, 1037–1044.
- [2] Mohammad Reza Bonyadi, Zbigniew Michalewicz, Markus Wagner, and Frank Neumann. 2019. Evolutionary computation for multicomponent problems: opportunities and future directions. In *Optimization in Industry*. Springer, 13–30.
- [3] Mohamed El Yafrani and Belaïd Ahiod. 2016. Population-based vs. single-solution heuristics for the travelling thief problem. In *Proceedings of the Genetic and Evolutionary Computation Conference 2016*. 317–324.
- [4] Mohamed El Yafrani and Belaïd Ahiod. 2017. A local search based approach for solving the Travelling Thief Problem: The pros and cons. *Applied Soft Computing* 52 (2017), 795–804.
- [5] Mohamed El Yafrani and Belaïd Ahiod. 2018. Efficiently solving the traveling thief problem using hill climbing and simulated annealing. *Information Sciences* 432 (2018), 231–244.
- [6] Mohamed El Yafrani, Marcella SR Martins, Mehdi El Krari, Markus Wagner, Myriam RBS Delgado, Belaïd Ahiod, and Ricardo Lüders. 2018. A fitness landscape analysis of the travelling thief problem. In *Proceedings of the Genetic and Evolutionary Computation Conference*. 277–284.
- [7] Edgar C Fieller and Egon S Pearson. 1961. Tests for rank correlation coefficients: II. *Biometrika* (1961), 29–40.
- [8] Mark D Humphries and Kevin Gurney. 2008. Network ‘small-world-ness’: a quantitative method for determining canonical network equivalence. *PLoS one* 3, 4 (2008), e0002051.
- [9] Domagoj Jakobovic, Stjepan Picek, Marcella S.R. Martins, and Markus Wagner. 2021. Toward more efficient heuristic construction of Boolean functions. *Applied Soft Computing* 107 (2021), 107327.
- [10] Yi Mei, Xiaodong Li, and Xin Yao. 2014. Improving efficiency of heuristics for the large scale traveling thief problem. In *Asia-Pacific Conference on Simulated Evolution and Learning*. Springer, 631–643.
- [11] Gabriela Ochoa, Marco Tomassini, Sébastien Vérel, and Christian Darabos. 2008. A study of NK landscapes’ basins and local optima networks. In *Proceedings of the 10th annual conference on Genetic and evolutionary computation*. 555–562.
- [12] Sergey Polyakovskiy, Mohammad Reza Bonyadi, Markus Wagner, Zbigniew Michalewicz, and Frank Neumann. 2014. A comprehensive benchmark set and heuristics for the traveling thief problem. In *Proceedings of the 2014 Annual Conference on Genetic and Evolutionary Computation*. 477–484.
- [13] Michal R Przybyłek, Adam Wierzbicki, and Zbigniew Michalewicz. 2018. Decomposition algorithms for a multi-hard problem. *Evolutionary computation* 26, 3 (2018), 507–533.
- [14] Markus Wagner. 2016. Stealing items more efficiently with ants: a swarm intelligence approach to the travelling thief problem. In *International Conference on Swarm Intelligence*. Springer, 273–281.
- [15] Junhua Wu, Sergey Polyakovskiy, and Frank Neumann. 2016. On the impact of the renting rate for the unconstrained nonlinear knapsack problem. In *Genetic and Evolutionary Computation Conference*. ACM, 413–419.
- [16] Rogier Hans Wuijts and Dirk Thierens. 2019. Investigation of the traveling thief problem. In *Proceedings of the Genetic and Evolutionary Computation Conference*. 329–337.